# Field Quality Study of a 1 m Long Single-Aperture 11 T $Nb_3Sn$ Dipole Model for LHC Upgrades

G. Chlachidze, J. DiMarco, N. Andreev, G. Apollinari, B. Auchmann, E. Barzi, R. Bossert, L. Fiscarelli, M. Karppinen, F. Nobrega, I. Novitski, L. Rossi, D. Smekens, D. Turrioni, G.V. Velev, A.V. Zlobin

***Abstract*— FNAL and CERN are carrying out a joint R&D program with the goal of building a 5.5-m long twin-aperture 11 T $Nb_3Sn$ dipole prototype suitable for installation in the LHC. An important part of the program is the development and test of a series of short single-aperture and twin-aperture dipole models with a nominal field of 11 T at the LHC operation current of 11.85 kA and 20% margin. This paper presents the results of magnetic measurements of a 1 m long single-aperture $Nb_3Sn$ dipole model fabricated and tested recently at FNAL including geometrical harmonics, and coil magnetization and iron saturation effects.**

***Index Terms*— Field quality, Magnetic Measurement, Superconducting accelerator magnets.**

## I. Introduction

THE planned upgrade of the Large Hadron Collider (LHC) collimation system foresees installation of additional collimators in the dispersion suppressor areas around points 2, 3 and 7 as well as around the high luminosity interaction regions [1]. Replacing some 8.33 T NbTi LHC main dipoles with shorter 11 T $Nb_3Sn$ dipoles compatible with the accelerator lattice and the LHC main systems could provide the required longitudinal space for the collimators. These twin-aperture dipoles operating at 1.9 K and powered in series with the main dipoles should deliver the same integrated strength of 119 Tm at the LHC operation current of 11.85 kA.

To demonstrate feasibility of this approach, CERN and FNAL have started in October 2010 a joint R&D program to build by 2015 a 5.5 m long twin-aperture $Nb_3Sn$ dipole prototype for the LHC collimation system upgrade. Two such cold masses with a collimator in between will replace one 14.3 m long LHC main dipole. The program started with the design and construction of a 2 m long single-aperture $Nb_3Sn$ demonstrator magnet [2] which was tested at FNAL in June 2012 [3]. To test new $Nb_3Sn$ strand and cable, improve the magnet quench performance and field quality, as well as to demonstrate performance reproducibility, the fabrication of four 1 m long collared coils was started at FNAL last year. These collared coils will be tested first in a single-aperture configuration and then assembled and tested inside a common iron yoke (twin-aperture configuration). In parallel, two 2 m long twin-aperture demonstrator dipole magnets will be built and tested at CERN to optimize the quench performance, field quality and quench protection of $Nb_3Sn$ coils and a somewhat different mechanical concept of the collar and yoke [4].

This paper presents the results of magnetic measurements of the first 1 m long single-aperture $Nb_3Sn$ dipole model MBHSP02 recently fabricated and tested at FNAL. The results and compared with results measured in MBHSP01 [5] including the geometrical harmonics, coil magnetization and iron saturation effects. Results of magnet quench performance and protection heater studies are reported elsewhere [6].

## II. Magnet Design and Parameters

The design concepts of 11 T $Nb_3Sn$ dipole in single-aperture and twin-aperture configurations are described in [2-4]. Magnet design is based on two-layer coils, collar and cold iron yoke supported by strong skin. The coil cross-section was optimized to provide a dipole field above 11 T at 11.85 kA in a 60 mm aperture, with ~20% margin on the load line at 1.9 K, and the low-order geometrical field harmonics below the $10^{-4}$ level. The coil has 6-block design and consists of 56 turns, 22 in the inner layer and 34 in the outer layer.

The details of the first 1 m long single-aperture dipole model MBHSP02 design and fabrication rpocedure are reported in [6, 7]. The single-aperture dipole cross-section is shown in Fig. 1.

Coils used in MBHSP02 were made of 40-strand 14.7 mm wide and 1.25 mm thick keystoned Rutherford cable with a stainless steel core and a new R&D strand [8]. The 0.025 mm thick and 11 mm wide core was used to reduce interstrand eddy currents in the cable. The 0.7 mm $Nb_3Sn$ RRP-150/169 strand has smaller sub-element size of ~35 μm to reduce the persistent current effect and improve cable stability with respect to the flux jumps. The cable was insulated with two layers of 0.075-mm thick and 12.7-mm wide E-glass tape.

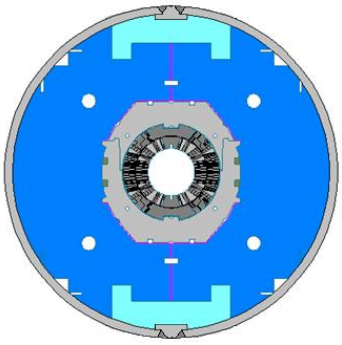

Fig. 1: Cold mass cross-sections.

Manuscript received July 16, 2013. Work supported by Fermi Research Alliance, LLC, under contract No. DE-AC02-07CH11359 with the U.S. Department of Energy and European Commission under FP7 project HiLumi LHC, GA no. 284404.

N. Andreev, G. Apollinari, E. Barzi, R. Bossert, G. Chlachidze, J. DiMarco, F. Nobrega, I. Novitski, D. Turrioni, G.V. Velev, A.V. Zlobin are with Fermi National Accelerator Laboratory, P.O. Box 500, Batavia, IL 60510, USA, (phone: 630-840-8192; fax: 630-840-8079; e-mail: zlobin@fnal.gov).

B. Auchmann, L. Fiscarelli, M. Karppinen, L. Rossi, D. Smekens are with the the European Organization for Nuclear Research, CERN CH-1211, Genève 23, Switzerland.

The coils, surrounded by a multi-layer Kapton insulation and 316L stainless steel protection shells, are placed inside the collar blocks made of high-Mn stainless steel. The collared coil is installed inside the vertically split 400 mm outer diameter yoke made of 1045 steel and fixed with aluminum clamps. The 12 mm thick 304L stainless steel skin provides final coil pre-compression and support. Two 50 mm thick 304L stainless steel end plates bolted to the skin restrict the longitudinal coil motion.

The calculated design parameters of the long single- and twin-aperture dipole magnets at $I_{nom}$ of 11.85 kA, $T_{op}$ of 1.9 K, nominal strand $J_c$(12T,4.2K) of 2750 A/mm$^2$ and cable $I_c$ degradation of 10% are shown in Table 1. For a 1 m long model in the single-aperture configuration, the calculated nominal parameters are slightly higher (for example, the field in magnet central cross-section is 11.07 T at $I_{nom}$=11.85 kA) due to field enhancement in the magnet straight section from the coil ends.

TABLE I
11 T DIPOLE PARAMETERS AT $I_{NOM}$.

| Parameter | Single-aperture | Twin-aperture |
|---|---|---|
| Yoke outer diameter, mm | 400 | 550 |
| Nominal bore field at $I_{nom}$, T | 10.88 | 11.23 |
| Short sample field $B_{SSL}$ at $T_{op}$, | 13.4 | 13.9 |
| Margin $B_{nom}/B_{SSL}$ at $T_{op}$, % | 81 | 83 |
| Stored energy at $I_{nom}$, kJ/m | 424 | 969 |
| $F_x$/quadrant at $I_{nom}$, MN/m | 2.89 | 3.16 |
| $F_y$/quadrant at $I_{nom}$, MN/m | -1.58 | -1.59 |

## III. MAGNETIC MEASUREMENT

Magnetic field in the aperture is expressed in terms of harmonic coefficients defined in a series expansion using the complex function formalism

$$B_y + iB_x = B_1 10^{-4} \sum_{n=1}^{\infty} (b_n + ia_n) \left( \frac{x+iy}{R_{ref}} \right)^{n-1} \quad (1)$$

where $B_x$ and $B_y$ in (1) are the horizontal and vertical field components in the Cartesian coordinates, $b_n$ and $a_n$ are the $2n$-pole normal and skew harmonic coefficients at the reference radius $R_{ref}$=17 mm. The right-handed measurement coordinate system is defined with the $z$-axis at the center of the magnet aperture and pointing from return to lead end.

The magnetic measurements were performed at the FNAL Vertical Magnet Test Facility using a new 130 mm long 16-layer Printed Circuit Board (PCB) probe [9]. The PCB probes and holder are shown in Fig. 2.

Fig.2. The Printed Circuit Board (PCB) with both 26-mm and 130-mm long, 28 mm in diameter probes (top) and PCB probe holder (bottom). Typical probe rotational speed is 1 Hz.

The new probe gives an increase in sensitivity by a factor of 10-15 over the 2-layer PCB probe used in the 2 m long demonstrator MBHSP01 [5]. A comparison is shown in Fig. 3. The new probe has both 130 mm and 26 mm long windings, the data of which are acquired simultaneously. The analog bucking achieved rejection of the main field by factors 850/470 for the 130/26 mm long windings respectively.

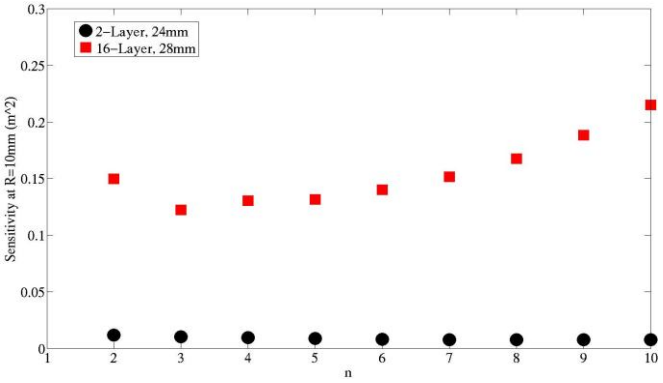


Fig. 3. Probe sensitivity comparison.

## IV. RESULTS AND DISCUSSION

### A. Coil Magnetization and Iron Saturation Effects

Figures 3-6 show the measured variations of the dipole transfer function (TF=$b_1$/I) and low-order normal ($b_3$, $b_5$) and skew ($a_3$) harmonics as a function of the excitation current. To estimate the effect of the eddy currents on the magnet transfer function and the field harmonics the measurements were performed at ramp rates of 10 A/s, 20 A/s, 40 A/s, and 80 A/s.

The large persistent current effect (hysteresis), seen at low currents in the *TF*, $b_3$ and $b_5$, is due to large $D_{eff}$ and $J_c$ of the used $Nb_3Sn$ strand. Some reduction of the persistent current effect, expected in MBHSP02 due to the smaller subelement size in RRP-150/169 strand, was compensated by the higher critical current density achieved in this strand during coil reaction.

The ramp rate effect in MBHSP02 is small as expected for the cored cable. The $a_3$ loops, in contrast to the 2 m long demonstrator MBHSP01 which showed tens of units in $a_3$ width, are less than 1 units.

The iron saturation is seen in *TF* and $b_3$. It starts at currents above 4 kA and is consistent with calculations for used iron and yoke geometry in the single-aperture configuration.

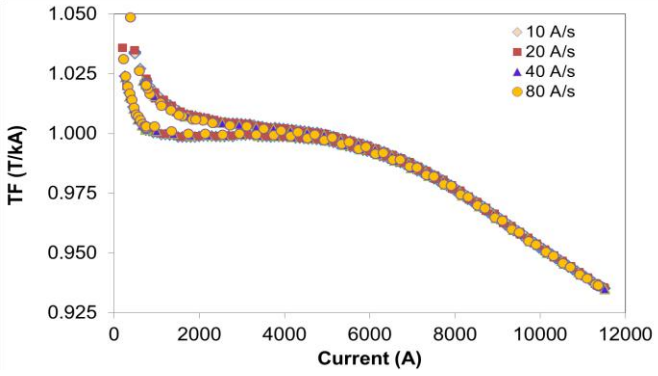


Fig. 3. Transfer function *TF* vs. magnet current.

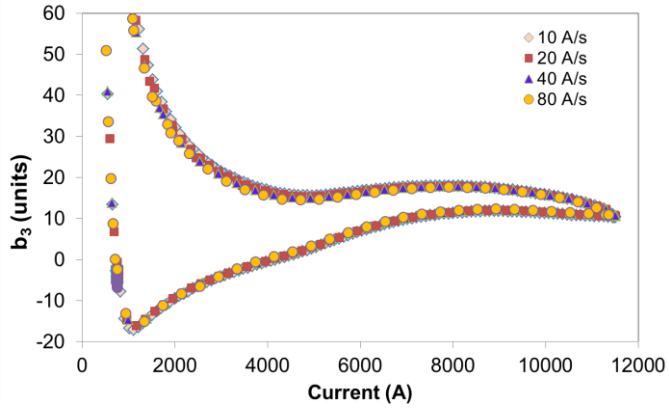


Fig. 4. Normal sextupole $b_3$ vs. magnet current.

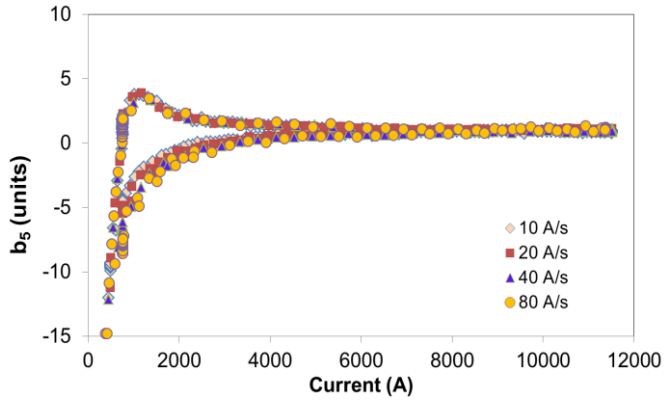


Fig. 5. Normal decapole $b_5$ vs. magnet current.

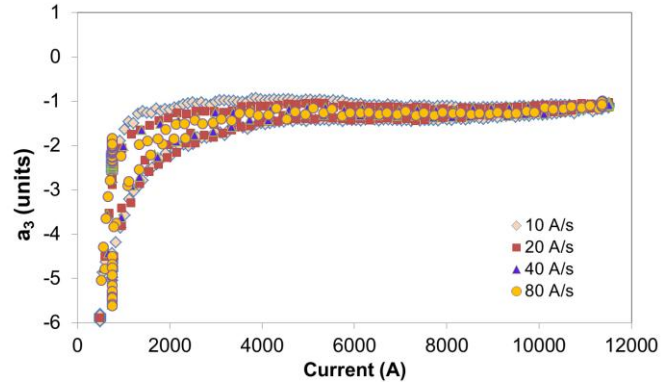


Fig. 6. Skew sextupole $a_3$ vs. magnet current.

## B. *Long-term Dynamic Effects*

Long-term dynamic effects in superconducting accelerator magnets are usually associated with the decay of the normal sextupole $b_3$ at injection, which is followed by a subsequent harmonics snapback during the acceleration ramp [10], [11]. Previous studies showed low level of these effects in $Nb_3Sn$ dipole and quadrupole models [12]. The measured $b_3$ decay in MBHSP01 was less than 2 units.

To determine these effects in the 1-m long dipole model MBHSP02, measurements were performed using an accelerator current profile similar to the one used in the LHC with the injection current of 0.76 kA, non-linear current ramp after injection and the nominal current of 11.5 kA. The duration of the injection plateau was set to ~900 s. The executed current profile is shown in Fig. 7.

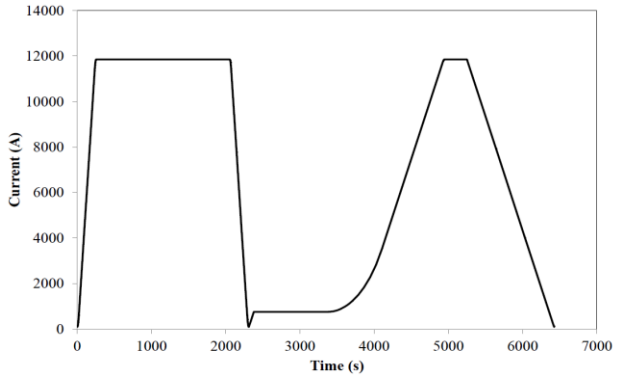


Fig. 7. Current profile of the accelerator cycle.

The decay and snapback effects in the normal sextupole component ($b_3$) are shown in Figures 8 and 9. The decay of the normal sextupole component at injection porch is ~8 units which is drastically larger than it has been measured in MBHSP01 [5]. Accelerator cycles were performed 3 times and it was found that the repeatability of the effect is very high - at the level of probe resolution. The cause of large dynamic effects observed in MBHSP02 needs to be understood.

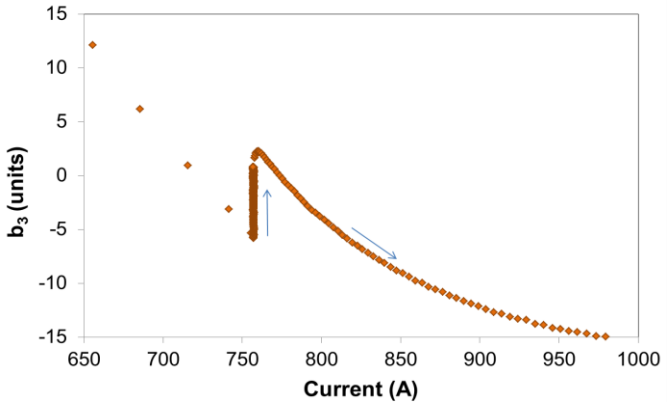


Fig. 8. Normal sextupole $b_3$ variation vs. current near the simulated injection plateau.

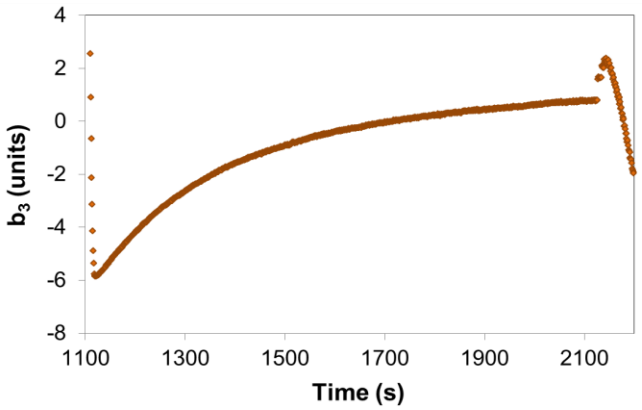


Fig. 9. Normal sextupole $b_3$ variation vs. time at the simulated injection plateau.

## C. *Effect of Temperature*

The LHC magnets are cooled by superfluid Helium at the temperature of 1.9 K. To investigate the effect of temperature on field harmonics a set of magnetic measurements were executed at 1.9 K and 4.5 K. The maximum magnet current

for these measurements was 11 kA and 9 kA respectively. In the current interval from 1 to 2 kA, the simulation using ROXIE code [13] predicts approximately 7% increase of the width of the hysteresis loop at 1.9 K due to higher critical current density $J_c$. However, the measurements in MBHSP01 showed 3% decrease in the $b_3$ hysteresis loop width. This discrepancy was further experimentally investigated in MBHSP02.

Figures 9 and 10 show the comparison of the transfer function *TF* and the normal sextupole $b_3$ measured at 4.5 K and 1.9 K. As in MBHSP01, the width of hysteresis loops in *TF* and $b_3$ at 4.5 K is the same or slightly larger than loop width at 1.9 K. This result suggests revision and improvement of the coil magnetization effects simulation model.

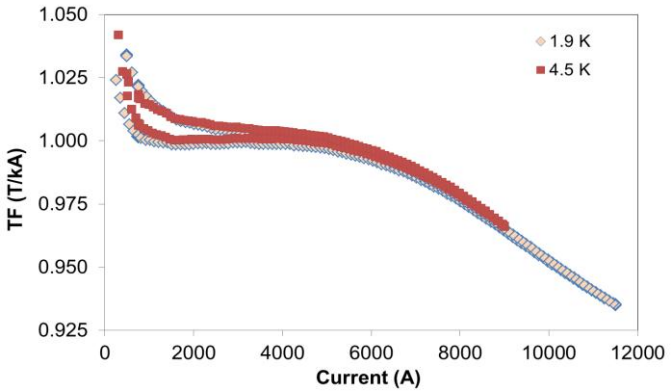


Fig. 10. Comparison of the transfer function measured at 1.9 and 4.5 K for 10 A/s current ramp.

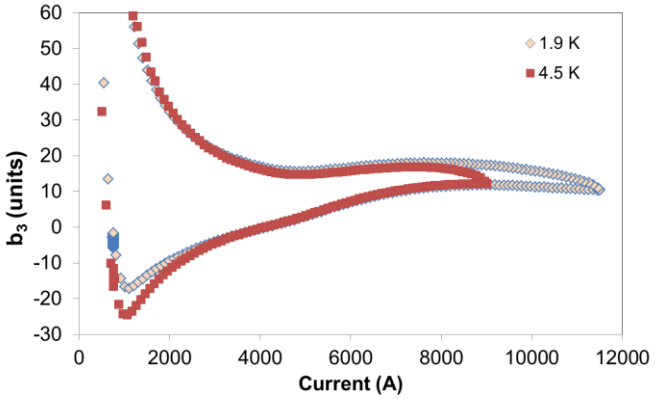


Fig. 9. Comparison of the sextupole field componenet measured at 1.9 and 4.5 K for 10 A/s current ramp.

### *D. Geometrical Harmonics*

Geometrical harmonics were defined by averaging the measured values at fixed current 3.5 kA during current ramp up and down. Table 2 presents the geometrical harmonics averaged over the probe length at the magnet current of 3.5 kA (before the iron saturation effect starts) for MBHSP02 which are compared with the design values [14] and measured values in MBHSP01 [5]. Significant improvement of the geometrical harmonics was achieved in MBHSP02 with respect to the MBHSP01. Still large values of $b_3$ and $a_3$ are likely due to the coil shimming used to achieve the required coil prestress. The large value of $b_2$ is due to the coil azimuthal misalignment inside the collar. Both effects will be optimized in the next models.

TABLE I
MEASURED GEOMETRICAL HARMONICS

| $b_n$, $a_n$ | Design | MBHSP01 | MBHSP02 |
|---|---|---|---|
| $b_2$ | 0.0 | -0.50 | -4.93 |
| $b_3$ | 0.3 | 6.38 | 8.44 |
| $b_4$ | 0.0 | 0.02 | -0.17 |
| $b_5$ | 0.9 | -0.73 | 1.02 |
| $b_6$ | 0.0 | 2.46 | -0.23 |
| $b_7$ | -0.1 | - | 0.03 |
| $b_9$ | 0.9 | - | 0.91 |
| $a_2$ | 0.0 | -1.43 | 0.14 |
| $a_3$ | 0.0 | 4.67 | -1.44 |
| $a_4$ | 0.0 | -2.50 | 0.24 |
| $a_5$ | 0.0 | 1.46 | 0.15 |
| $a_6$ | 0.0 | -2.32 | 0.00 |
| $a_7$ | 0.0 | - | -0.05 |
| $a_9$ | 0.0 | - | 0.34 |

## V. CONCLUSION

Magnetic measurements were performed for the 1 m long single-aperture 11 T dipole model including geometrical harmonics, coil magnetization and iron saturation effects.

The design geometrical field harmonics in the magnet body have been notably reduced by coil cross-section optimization. However, some measured low order harmonics are still quite large due to the imperfect "as-built" coil geometry. The level of geometrical harmonics will be reduced in the future by optimizing the coil geometry taking into account the above effects.

The iron saturation effect in the single-aperture configuration was measured in the whole operation current range and is well understood.

The persistent current effect is relatively large at the LHC injection level due to the high $J_c$ and large $D_{\text{eff}}$ in the present $Nb_3Sn$ strands. If necessary, this effect could be reduced using special passive correction schemes. The eddy current effect in TF and all allowed and non-allowed harmonics was suppressed by using a stainless steel core inside the cable.

The dynamic effects in the normal sextupole component observed in this model are quite large, the $b_3$ decay is around 8 units. The cause of large dynamic effects observed in MBHSP02 needs to be understood.

## ACKNOWLEDGMENT

The authors thank technical staff of FNAL Technical Division for contributions to magnet design and fabrication.

## REFERENCES

[1] L. Bottura et al., "Advanced Accelerator Magnets for Upgrading the LHC", IEEE Trans. on Applied Supercond., Vol. 22, Issue 3, 2012, p. 4002008.

[2] A.V. Zlobin et al., "Development of $Nb_3Sn$ 11 T Single Aperture Demonstrator Dipole for LHC Upgrades", Proc. of PAC'2011, NYC, 2011, p. 1460.

[3] A.V. Zlobin et al., "Development and test of a single-aperture 11T $Nb_3Sn$ demonstrator dipole for LHC upgrades", IEEE Trans. on Appl. Supercond., Vol. 23, N 3, 2013, p. 4000904.

[4] M. Karppinen et al., "Design of 11 T Twin-Aperture $Nb_3Sn$ Dipole Demonstrator Magnet for LHC Upgrades", IEEE Trans. on Appl. Supercond., Vol. 22, N 3, 2012, p. 4901504.

[5] N. Andreev et al., “Field Quality Measurements in a Single-Aperture 11T $Nb_3Sn$ Demonstrator Dipole for LHC Upgrades”, IEEE Trans. on Appl. Supercond., Vol. 23, Issue 3, June 2013 Page 4001804.
[6] A.V. Zlobin et al., “Quench Performance of a 1 m Long Single-Aperture 11 T $Nb_3Sn$ Dipole Model for LHC Upgrades”, *this conference.*
[7] A.V. Zlobin et al., “Fabrication and Test of a 1-m Long Single-Aperture 11T $Nb_3Sn$ Dipole for LHC Upgrades”, Proc. of IPAC’2013, Shanghai, China, May 2013, p. 3609.
[8] E. Barzi et al., “Superconducting Strand and Cable Development for the LHC Upgrades and Beyond,” IEEE Trans. on Appl. Supercond., Vol. 23, Issue 3, 2013, p. 6001112.
[9] J. DiMarco et al., “Application of PCB and FDM Technologies to Magnetic Measurement Probe System Development”, IEEE Trans. on Appl. Supercond., Vol. 23, Issue 3, 2013, p. 9000505.
[10] N. Sammut et al., “Mathematical Formulation to Predict the Harmonics of the Superconducting Large Hadron Collider Magnets: II. Dynamic field changes and scaling laws” Phys. Rev. Spec. Top. Accel. Beams 10, 2007.
[11] G.V. Velev *et al*., “Measurements of the Persistent Current Decay and Snapback Effect in Tevatron Dipole”, *IEEE Trans. Appl. Supercond*., vol. 17, 2007, pp. 1105-1108.
[12] G.V. Velev *et al.,* “Measurements of the Persistent Current Decay and Snapback Effect in $Nb_3Sn$ Accelerator Prototype Magnets at Fermilab”, *Proc. of IPAC2012*, New Orleans, 2012, p. 3593.
[13] ROXIE code for an electromagnetic simulation and optimization of accelerator magnets, http://cern.ch/roxie.
[14] B. Auchmann et al., “Field Quality Analysis of a Single-Aperture 11T $Nb_3Sn$ Demonstrator Dipole for LHC Upgrades”, Proc. of IPAC2012, New Orleans, 2012, p. 3596.